Modelling biological invasions: species traits, species interactions, and habitat heterogeneity

Sergio A. Cannas[1,2], Diana E. Marco[3], Sergio A. Páez[4]

1– Facultad de Matemática, Astronomía y Física, Universidad Nacional de Córdoba, Ciudad Universitaria, 5000 Córdoba, Argentina.

2– Corresponding author. Fax: +54 351 4334054. e-mail: cannas@famaf.unc.edu.ar.

3– Facultad de Ciencias Agropecuarias, Universidad Católica de Córdoba, 5000 Córdoba, Argentina.

4– INTA, EEA Bariloche, Pasaje Villa Verde S/N, CC 277, 8400 San Carlos de Bariloche, Argentina.

Abstract

In this paper we explore the integration of different factors to understand, predict and control ecological invasions, through a general cellular automaton model especially developed. The model includes life history traits of several species in a modular structure (Interacting Multiple Cellular Automata, IMCA). We performed simulations using field values corresponding to the exotic *Gleditsia triacanthos* and native co-dominant trees in a montane area. Presence of *G. triacanthos* juvenile bank was a determinant condition for invasion success. Main parameters influencing invasion velocity were mean seed dispersal distance and minimum reproductive age. Seed production had a small influence on the invasion velocity. Velocities predicted by the model agreed well with estimations from field data. Values of population density predicted matched field values closely. The modular structure of the model, the explicit interaction between the invader and the native species, and the simplicity of parameters and transition rules are novel features of the model.

Keywords Biological invasions, cellular automata, invaders, habitat heterogeneity, species interaction.

Introduction

Organisms spreading outside of their native ranges have been called "invaders". The process by which an invader arrives and spreads into the new territory is called "ecological invasion", and has been recognised as potentially damaging for ecosystems functioning since Elton's work [1]. Since this early treatise some interesting although fragmentary advances to explain invasion success have been made by addressing the idea that the spread of an invasive alien organism in a natural system depends on different factors, like life history and demographic traits of the alien species, and environmental conditions of the invasion system, including disturbance regime (citations in [2]-[3]). Interspecific interactions between the alien and the native species, another important factor, have rarely been considered [4]-[5].

However, this increasing theoretical knowledge has not been translated yet into the development of effective control programs, and prediction of the fate of invasions once the invader has arrived is still as far to reach as stated by Gilpin [6] in 1990: "we are never going to have a scheme to predict the success of invading species". Reasons for this failure could be related to the largely anecdotical nature of the invasion data gathered in different systems, the biased nature of many studies, and the lack of integration of invaders traits and environmental (including native species) characteristics. We believe that integration of the different factors involved in invasion processes by formalisation through mathematical models [7], is the most fructiferous approach to understand, predict and control ecological invasions. Moreover, there is a particular kind of mathematical models that is especially suitable for modelling the invasion process: the cellular automata, since they permit to easily incorporate the different factors involved in the invasions in a spatially explicit context. This

feature has proven to confer cellular automata a better simulation properties compared to the classic reaction-difussion model used in the invasion studies since Skellam [8] and Okubo [9] applications [7] [10]. In this paper we describe a general cellular automaton model developed for studying invasions. Our model represents an improvement respect to the other few cellular automata models for invasions reported in the literature [11]-[14], because it considers the demography of the invader and the native species, how the interspecific interaction between them affects the invasion dynamics, and permits to simulate an ample range of invasion processes.

The Model

We develop an individual based cellular automaton model for the population dynamics and spatial spread of a single isolated species. The model takes into account the life history traits of the species relevant to species dynamics. To include interaction between species, we develop a similar model for each one including the corresponding set of life history traits. We then define dynamical interacting rules that couple the variables associated to each cellular automaton. We call this last model version an Interacting Multiple Cellular Automata (IMCA). Models based on cellular automata are usually defined by associating to every cell of a grid a single discrete variable, which values encode all the possible states of the cell. For instance, in the case of modelling a single species the variable may encode the age of the individual at the cell [11], or in the case of several species, each value can be associated to the presence of an individual belonging to a different species. In the IMCA we associate to every cell in the grid *several* discrete variables [15], each one encoding the age of an individual belonging to a different species. This approach allows to model in a clear and

simple way systems of increasing complexity. Dynamical properties inherent to every species are incorporated separately from the interaction factors, thus allowing to develop a "modular strategy" of modelling, where the building blocks are relatively simple one species cellular automata models.

We performed several simulations using field values corresponding to *Gleditsia triacanthos* L.and *Lithraea ternifolia* (Gill) Barkley [10] and *Fagara coco* (Gill) Engl [16]. Using the simulation results we calculated the temporal behavior of average population densities and propagation fronts, from which we obtained an estimation of the invasion velocity of *G. triacanthos* in a dense forest of *L. ternifolia*. We also analised the dynamics of a mixed forest of the two native, non-invasive species *L. ternifolia* and *F. coco*. In this simulation we expected the model predicting stable coexistence of the two species in the long term.

One species cellular automaton

We embed the model on a square grid containing $L_x \times L_y$ cells. The grid parameter (i.e., the distance between neighbouring cells) equals one. We choose the spatial length scale so that each cell contains at most one adult individual. We consider a discrete time unit and the dynamical variables are updated according to a parallel dynamics, that is, the value of all variables at a given time t depends on the value of the variables at time $t-1$. We set the time scale to coincide with the minimal reproductive interval in the life history of the species. Throughout the paper, time unit is then one year. Life history traits considered are: d, mean seed dispersal distance (in grid units), t_{max}, maximum longevity (in years), q, annual adult survival probability (calculated from t_{max}), t_m, age of reproductive maturity (in years), n, mean seed production (seeds/plant), t_s, interval between masting seed crops (in

years), f_g, mean germination probability, P_s, juvenile survival probability, and a_J, average age of saplings in the juvenile bank (in years). Juvenile bank is the collection of saplings that germinate under closed canopy and can survive in the shade, ageing but not growing, until a gap in the canopy appears and saplings can resume their growth and eventually reproduce [17].

Each cell i have associated a discrete variable $a_i(t)$ corresponding to the *age* of the individual located at it at time t; $a_i = 0$ corresponds to an empty cell. The index i encodes a pair of discrete coordinates (x, y), with $x = 1, 2, \ldots, L_x$, $y = 1, 2, \ldots, L_y$.

An occupied site $a_i(t) \neq 0$ is updated according to the following rule:

$$a_i(t+1) = \begin{cases} a_i(t) + 1 & with \quad probability \quad q \\ 0 & with \quad probability \quad 1-q \end{cases} \tag{1}$$

where q is the annual *adult survival probability*. We chose the value of the parameter q as follows. Since at every year the survival of an individual is sorted independently, the probability $P_d(t)$ that an individual dies at age t is given by a geometrical distribution

$$P_d(t) = (1-q)q^{t-1}. \tag{2}$$

Let t_{max} be the maximum longevity of the species. From Eq.(2) we can calculate the probability of an individual to survive over t_{max} as

$$\begin{aligned} P(t > t_{max}) &= 1 - \sum_{t=1}^{t_{max}} P_d(t) \\ &= 1 - \frac{1 - q^{t_{max}+1}}{q}. \end{aligned} \tag{3}$$

Using Eq.(3) we choose q so that $P(t > t_{max}) < 0.05$.

Let t_J be the average age of the juvenile bank of the species. If the individual dies at time t, i.e., $a_i(t-1) \neq 0$ and $a_i(t) = 0$, it is replaced by another individual of age t_J. If the species does not have juvenile bank then $t_J = 0$ and the cell becomes empty.

Now consider an empty cell i at time $t-1$, that is, $a_i(t-1) = 0$. The site will be colonised at time t, that is, $a_i(t) = 1$ with probability $p_i(t)$. The *colonisation probability* $p_i(t)$ depends on the number of seeds $s_i(t)$ received by the cell i at time t, and it is defined as the probability that *at least* one seed germinates *and* that the corresponding individual survives to the adult stage (more than two years). Let f_g be the mean germination probability of the species and P_s the probability that a juvenile survives more than two years. Considering these two events as independent lead us to

$$p_i = 1 - (1 - P_s f_g)^{s_i} \tag{4}$$

To calculate s_i we count the seeds received by the cell i coming from the rest of the cells. Let us assume that the seeds dispersion of an individual is described by some density function $f(r)$, where $r = \sqrt{x^2 + y^2}$ is the distance to the parental tree. That is, we assume that seed dispersion is spatially isotropic. This assumption is not restrictive and it can be easily generalised to consider anisotropic seed distributions. The function $f(r)$ describes the fraction of the total number of seeds produced by a single individual that are dispersed per unit of area to a distance r; $f(r)$ is assumed to be normalized in the whole plane. Now the fraction of seeds received by a cell j coming from an individual located at a cell i is given by

$$K(r_{ij}) = \int_{\Omega_j} f(r) da \tag{5}$$

where the integration variable r is the distance to the center of the cell i, Ω_j is the area of the cell j and r_{ij} is the distance between the center of the cells i and j. The integrals (5) must be in principle carried out over the all the area Ω_j. However, for a wide range of different choices of $f(r)$ the above integral can be well approximated as $K(r_{i,j}) \approx f(r_{ij})$. Then s_i is obtained as $s_i(t) = n\, g_i(t)$, where

$$g_i(t) = \sum_{i \neq j} K(r_{ij}) \Theta\left(a_j(t-1) - t_m\right) \Lambda\left(a_j(t-1) - t_m, t_s\right) \tag{6}$$

where the sum runs over all cells $j \neq i$, the step function $\Theta(x)$ is defined as

$$\Theta(x) \begin{cases} 1 & if \quad x > 0 \\ 0 & if \quad x \leq 0 \end{cases} \tag{7}$$

and $\Lambda(x, y)$ is a function that equals one if x is a multiple of y and zero otherwise. That is, an individual located at the cell j will contribute with $nK(r_{ij})$ seeds to the cell i every t_s years starting from $a_j = t_m$. In the case of annual seed crops $t_s = 1$ (*i.e.*, no masting seed crops) we have that $\Lambda(x, 1) = 1\ \forall x$.

Interacting Multiple Cellular Automata (IMCA)

To work with several species we incorporate interactions between them by coupling the cellular automata through dynamical interacting rules. For simplicity, we will refer to a "success" of a species when it can colonise a new grid cell, and to a "winner" when a species outcompete another during the interacting process. Unless a particular resource is explicitly

considered, competition occurs in an ample sense as competition by space. The interacting rules are the following:

1. A given cell cannot be occupied by individuals of different species at the same time.

2. In an empty cell we compute the probability of colonisation by different species from Eq.(4) and compare them with independent random numbers sorted for each one. If only one species succeeds the dynamics is that of a single species. If more than one species succeed the winner is sorted with some probability that depends on the particular set of species under consideration. If all the species make a similar use of the environmental resources then the winner is sorted with equal probability among the occurring species at the cell.

3. If different species make different use of the environmental resources then new parameters are incorporated into the model. Consider for instance the case of two species, where one of them has a especial ability to establish in shallow soils and rock crevices compared to the other. We introduce a soil state parameter c_i for each cell i, which can take the values 0 and 1, representing a rocky ground and a deep soil cell, respectively. These parameters are sorted with some spatial distribution at the beginning of the simulation and kept fixed through it. We introduce the following competition rule: if $c_i = 1$ the winner is sorted with equal probability but, if $c_i = 0$, then the species with the especial ability soil occupation always succeeds in colonising the cell.

Simulation Methods

We performed computer simulations of the spread of different species. First we simulated the behaviour of isolated species and then we analise the interacting situation for different combinations of pairs of species. In most of the cases the results were averaged over many samples of random initial conditions and also over different sets of the random numbers used in the dynamics. We considered open boundary conditions, that is, cells do not receive seeds from outside the grid area. Initially, we simulated the isolated spread of each *L. ternifolia*, *G. triacanthos* and *F. coco* species in an empty rectangular area, starting from a row of individuals along a line $y = 0$ at the bottom of the rectangle. We chose the age of the individuals randomly between 1 and t_m. The cell length unit is 5 m, corresponding to an average adult canopy ($25m^2$) of the species considered. We chose the seed dispersal distribution as a negative exponential function

$$f(r) = \frac{2}{\pi d^2} e^{-2r/d} \tag{8}$$

Values of the life history traits are in Table 1. The propagation front $y = h(x)$ for each species was defined as the farthest occupied cell y from the starting point for every coordinate x. We defined the mean front position as

$$\overline{h} = \frac{1}{L_x} \sum_{x=1}^{L_x} h(x) \tag{9}$$

We averaged $\overline{h}$ over different initial conditions and different sets of random numbers, for all species, for an area of width $L_x = 80$. Several tests performed for different area width showed that the results did not change significatively for widths over 80 cells.

To gain a deeper insight about the invasion front structure we also calculated the invader

population denstity profiles along the propagation direction y:

$$\rho_1(y,t) = \frac{1}{L_x}\sum_{x=1}^{L_x}\left[\Theta\left(a_{x,y}(t)\right) - \Theta\left(a_{x,y}(t) - t_m\right)\right] \quad (10)$$

$$\rho_2(y,t) = \frac{1}{L_x}\sum_{x=1}^{L_x}\Theta\left(a_{x,y}(t) - t_m\right) \quad (11)$$

where $a_{x,y}$ is the age of an invader located at a cell whose coordinates in the grid are (x, y) and $\Theta(x)$ is given by Eq.(7); ρ_1 and ρ_2 give us the average density profiles for non-reproductive and reproductive individuals respectively.

We first used the IMCA to study the invasion system constituted by the alien species *G. triacanthos* and the native dominant *L. ternifolia*. Using the life history traits values in Table 1, and the interacting rules previously defined, we simulated the spread of *G. triacanthos* on a rectangular area, starting from an initial distribution of individuals with random ages along a line $y = 0$ at the bottom of the rectangle. We filled the rectangle with a dense forest of *L. ternifolia* individuals of random ages. We can characterise the time evolution of the invasion patterns by defining the invasion front $y = h(x)$ as the farthest cell occupied by *G. triacanthos* for every coordinate x, as in the non interacting case. We performed another set of simulations, starting from a single *G. triacanthos* tree located in the centre of a square area covered by a dense forest of *L. ternifolia*. We also studied the spread of *F. coco* in the presence of *L. ternifolia* forest, using the life history parameters given in Table 1. Since both species make a similar use of the habitat, no soil variables were introduced in this case. As in the previous simulations we started considering the spread in a rectangular area from an initial linear distribution of individuals randomly aged of *F. coco* at the bottom of the area. We filled the area with a dense forest of *L. ternifolia*. We performed another

set of simulations, by initially filling the grid with a randomly interspersed distribution of individuals of *F. coco* and *L. ternifolia*, in different percentages.

Results

Single species spread

In all simulations performed, $\overline{h}$ shows, after a transient period, a linear behaviour $\overline{h} \sim Vt$, with a well defined asymptotic velocity V. This holds as long as the spread front does not reach the upper border of the area $y = L_y$, where the population densities stabilise at values between 0.9 and 1 in all cases. For the sake of comparison we also simulated the spread of starting from a single tree located in the centre of the area. The spread front in this case develops an almost circular shape (not shown), which average asymptotic velocity is the same of that obtained using the previous initial linear distribution of trees. Asymptotic velocities predicted by the model were 9.6 m/y for *G. triacanthos*, 0.6 m/y for *L. ternifolia*, and 3.3 m/y for *F. coco*. In all cases, the propagation front $h(x)$ is relatively smooth (not shown).

In figure 1 we show the density profiles for *G. triacanthos* propagation at three different times; the profiles for other species behave in an analogous way. We see that the profiles display a "travelling wave" structure, that is, they satisfy the property $\rho(y, t+n) = \rho(y-nV, t)$ $(n = 1, 2, \ldots)$, as can be appreciated from figure 2. We can also see from figure 2 that the travelling wave fronts present asymptotically an exponential tail for large times, consistent with the prediction of integro-difference models for structured populations of Neubert and Caswell [18]. It is worth noting in figure 1 the presence of a wide band of non-reproductive individu-

als in the invasion front, characterized by a sharp peak in the corresponding density profile. We see that about half of the area covered by the front is composed by non-reproductive individuals. Moreover, the width of this area (about 20 grid units) is much more larger than the mean dispersal distance ($d = 3$ grid units in this example), which means that the front advances only when non-reproductive individuals in the front become reproductive.

Interacting species

In Fig.3 we show an example of snapshots of the spread of *G. triacanthos* into the dense *L. ternifolia* forest, in homogeneously deep soil ($c_i = 1$ for each cell i). In this interacting case, the smooth front characteristic of the single species spread, is replaced by a wide spread band area of rough borders, as the result of the intermingled patches of *G. triacanthos* invading *L. ternifolia* forest. Inside the invasion band, that move along the y axis direction, there are many patches of *L. ternifolia* of different sizes. These *L. ternifolia* patches are replaced by *G. triacanthos* as the simulation runs, leaving a dense forest of the invader behind the band. After some time the whole area is invaded by *G. triacanthos*. This can be seen in Fig.4, where we plotted the average population densities (number of individuals/total area) *vs* time for both species. In the case of *G. triacanthos* beginning to spread into *L. ternifolia* forest from a single tree located in the centre of the squared area, the invasion band growing radially shows the same characteristics as in the linear initial start.

To estimate the velocity of the invasion process we use the asymptotic speed V of the averaged front position $\overline{h}$. In Fig.5 we show the temporal behaviour of $\overline{h}$ for two different soil states, homogeneously deep soil ($c_i = 1$ for each cell i), and homogeneously rocky ground ($c_i = 0$ for each cell i). Again we see that $\overline{h}$ displays a well defined asymptotic linear

behaviour in both cases. Although on rocky ground the process is much more slower, *G. triacanthos* always succeeds in the invasion into the *L. ternifolia* forest. We checked for the validity of simulations, comparing rates of spread predicted by the model with data obtained from aerial photographs 1:5000, taken in the study area in 1970, 1987 and 1996. The last velocity was estimated from the increment in the square root of the whole invaded area. Velocity estimated from photographs is 2.4 m/y, while velocity predicted by the model ranges from 1.9 m/y in rocky ground to 4.4 m/y in deep soil (Fig.5). We also performed simulations with a random distribution of rocky ground and deep soil cells in different proportions. The results (not shown) are qualitatively the same as in Fig. 5, with velocities that vary between the two values shown in the figure. We then calculated the invasion profiles ρ_1 and ρ_2 (see Eqs.(10) and (11)) for the invasion of *G. triacanthos* in a dense forest of *L. ternifolia*. The results are shown in Fig.6. We see that the profiles show a travelling wave structure as in the non-interactive case. Moreover, it can be seen that the travelling wave fronts also present an exponential tail at large times. A similar behaviour is encountered in the solutions of integro-difference models for invasion systems that include short-range seed dispersal and competition between aliens and natives, as far as competition favours the invader [19] (in the present case the existence of juvenile bank gives a formidable advantage to the invader). Comparing figures 1 and 6 we see that the presence of native competitor completely supress the peak in the non-reproductive travelling wave front that appears in the non-interactive case.

When considering the interacting case between the two natives *L. ternifolia* and *F. coco*, the spread of *F. coco* into the *L. ternifolia* forest does not lead to exclusion of *L. ternifolia*. As long as *F. coco* spreads into the area, cells behind the spreading front can be re-occupied

by *L. ternifolia*. This leads, after some time, to a stationary situation of a mixed forest with a distribution of patches of both species (Fig.7). Starting from an initial random mixing of both species, after some time the system attains a stationary state with fixed values for the average population density values of both native species (not shown). Such values do not depend on the initial values, as shown in Fig. 8. Moreover, the predicted proportion between the stationary densities: number of individuals of *L. ternifolia*/number of individuals of *F. coco* $= 0.67/0.29 \approx 2.3$ compares well with the field data value 2 ± 1 [16].

In order to elucidate the influence of the juvenile bank in the invasion process we performed another simulation of the *L. ternifolia*-*G. triacanthos* system, but withdrawing the juvenile bank of *G. triacanthos*. In this case the dynamics of the model led to a final situation very similar to that observed in the *L. ternifolia*-*F. coco* system, with a different stationary densities ratio (the number of individuals of *G. triacanthos* is about the same of that of *L. ternifolia*). In other words, in this case there is no invasion but coexistence, at least for the particular set of values of the parameters here considered. This shows that the juvenile bank is a determinant factor in the succes of *G. triacanthos* invasion in this system. It is worth mention that a sensitivity analysis showed that the invasion velocity was not influenced by variations of the age of juvenile saplings t_J. Further simulations, using the set of parameters of *G. triacanthos* without juvenile bank for the invader and the set of parameters of *L. ternifolia* for the native, showed that, for values of the native longevity comparables to that of the invader, the native may become extinct at large times, even in the absence of the juvenile bank. Finally, in order to determine the sensitivity of the invasion velocity with the life history parameters, we performed a certain number of simulations changing the values of different life history parameters while keeping the rest of them fixed, for different

combinations of species.

First of all, we observed that for an invader with juvenile bank, the invasion velocity in a dense forest of natives (the situation we simulated in this work) is almost independent on all the life history parameters of the native but the longevity. In this case the behavior of the native can be very well aproximated by a simplified version of the one species CA model (see Fig.9), which is obtained as the $n \to \infty$ and/or $P_s f_g \to 1$ limit ; in such limit we see from Eq.(4) that the colonization probability $p_i = 1$ independently of the cell i, leading to a Non-Interacting (NI) model. Hence, the dynamics of the native depends in this case only on the survival probability q_n, which is related to the longevity through Eq.(3). This property holds only if the invader has a juvenile bank.

We then calculated the variation of the invasion velocity V with the mean dispersal distance d, for an invader with juvenile bank and for different values of the age of reproductive maturity t_m while keeping all the rest of the parameters fixed with values corresponding to *G. triacanthos* . From Fig.10 we see that V depends linearly on d. From the same calculation it can be seen that V decays logarithmically with t_m for small values of it ($t_m < 7y$) ; for higher values of t_m we found that $V \sim 1/t_m$ (not shown).

We next calculated the variation of V with the mean seed production n while keeping d and t_m fixed. In Fig.11a we present a calculation of V as a function of n for different values of the product $P_s f_g$; we see from the normal-log plot that V grows logarithmically with n, at least for large values of n. Moreover, since the velocity invasion is determined by the colonisation probabilities p_i, which can be written as $p_i = 1 - A^{g_i(t)}$ (see Eq.(4)), we see that the velocity depends on n through the factor $A = (1 - P_s f_g)^n$. The data collapse of the curves from Fig.11a shown in Fig.11b, when we plot V vs $-nLn(1 - P_s f_g) = -Ln(A)$,

shows that actually $V \sim Ln(-Ln(A))$.

Discussion

The most important factor determining invasion success detected by the IMCA model is the presence of a juvenile bank. Once a cell is occupied by *G. triacanthos* or *L. lucidum*, the native *L. ternifolia* cannot enter on it anymore, because even when the adult invader individual deads, it leaves on the site a collection of saplings ready to resume growth and reproduce. The juvenile bank thus represents an effective strategy for ensuring site occupancy. This strategy is comparable with the "phalanx growth strategy" that occurs when a species shows either a clonal growth in a compact manner [20], or the species makes the neighbourhood uninvadable by species with shade-tolerant seedlings as in the case of *G. triacanthos* and *L lucidum*, conferring them an invasive ability as space-holder invaders [21]. However, in contrast with the conditions settled for these authors for the phalanx growth strategy to apply (resident native species with global dispersal and invader with local dispersal), we found the phalanx strategy in the case of both native and invader species showing local disperse. The role of the juvenile bank in the invasion success can be paralleled to the role of the seed bank, especially for short-lived invaders. Many invasive weeds depend on seed banks for persistence in seminatural habitats [22].

Respect to the relevant parameters influencing invasion velocity, we found that the main ones are the mean dispersal distance d and the age of first reproduction t_m, while it changes slowly (logarithmically) with the number of seeds n. We showed that the model predicts a wave form structure for the invasion front, both for the non-interactive and interactive cases. However, the detailed structure of the front is very different in both cases. In the non-

interactive cases the front presents a sharp peak in the non-reproductive population density, followed by the wave of reproductive individuals, behaviour that is not present in the integro-difference models solutions [18]. The situation is quite different in the interactive case, where the travelling wave front is mostly composed by reproductive individuals. Moreover, we found that in the case of invader species with juvenile bank, the invasion velocity is almost independent of the life history parameters of the native except adult survival probability q_n. This can be easily understood since the basic mechanism underlying the front motion in this case is colonization of random neighboring gaps, whose production rate is proportional to $1 - q_n$.

Mean dispersal distance was important in determining invasion velocity. It is worth noting that all the simulation were performed using a negative exponential function as the seed dispersal curve, allowing for short distance dispersal only. The choice of the dispersal function was based on the lack of evidence for long distance dispersal events for the species here considered in the habitat analyzed. Invasion velocity increased linearly with increasing d, as expected for a dispersal distribution function which has a moment-generating function [23], like the exponential here used. With a well defined invasion travelling wave and local dispersal the invasion processes described by the IMCA model are qualitatively analogous to those obtained from applications of the reaction-diffusion model [11, 10], integro-difference equation models [19, 24, 25] or the model coupling integro-difference equations with population matrices developed by Neubert and Caswell [18]. On the other hand, when fat-tailed desipersal curves fucntions are considered, accelerated invasions are produced [23, 24, 26]. If necessary, suitable fat-tailed dispersal functions like the Cauchy distribution [23] can be easily incorporated into the IMCA model.

Minimum reproductive age was one of the main predictors of invasive pines and woody angiosperms around the world [27]. Looking at the population age structure of the travelling invasion wave when considering short range dispersal it is evident that the invasion advances only when the non-reproductive individuals located in the invasion front reach the reproductive maturity (see Fig. 1). Under these conditions, the basic mechanism underlying the motion of invasion front is diffusion, where the relevant time scale involved is the age of reproductive maturity t_m. This is consistent with the analytic results of Kot et al [23], showing that the minimum speed of a moving invasion wave when using integro-difference equation models depends on the net reproductive rate R_0. Short reproductive periods mean shorter generation times T, and hence, greater R_0 . The other component of of R_0, fecundity (as seed production, for example) is perhaps less important in determining invasion velocity. Seed production has not influenced primarily the invasion velocity in the IMCA, at least for reasonable values of seed prodeuction n. Fecundity as seed production is difficult to be limiting for population growth in plants, being of the order of hundreds or thousands [28]. It is interesting to note that, even in the case when long-distance dispersal was considered by using fat-tailed distributions, the mean rate of population spread was given by the density at extreme distances reached by teh farthest individuals scaled by the generation time T [29]. Moreover, juvenile survivorship was decisive for determining spread velocity in the model from Clark et al [29], rather than seed production. This is consistent with other findings for woody species, where survival transitions are more important than fecundity in determining population growth rates [17]. Such generalisation is supported by an independent application of matrices models on the same system tested in the IMCA [10], where seed production made the lowest contribution to population growth of *G. triacanthos*. This could explain in

part why *Eucalyptus* species have not been as successful invaders as could be expected from their large seed production [30]. However, seed production could be more important than survival transitions when invaders are short-lived species, as found by [31] for the short-lived perennial *Senecio jacobaea*. As long as in most of studies fecundity measurements involve both seed production and seedling survival or even ignore seed production [27]; [11], the importance of the two factors in promoting invasion success is difficult to assess. An interesting way of assessing this importance is the finding of Neubert and Caswell [18] that the sensitivity patterns of both population growth and invasion wave speed are similar.

The IMCA model permits to integrate explicitely the effects of the invader and the native species interactions on their demography, and hence, on the invasion success. In the case analysed, interaction between invader and native species was related to the use of resources through competition leading to a decrease of the invasion velocity, but any kind of ecological interactions and relationships with the environment, including disturbances, can be modeled very easily using IMCA. This confers the model a great flexibility and generalisation power, in contrast to the formerly used reaction-diffusion model. The predicted rates of invasion for *G. triacanthos* using the reaction-diffusion model in the same invasion system described in this paper [10], have been overestimated in an order of magnitude compared to the results of the IMCA. In the IMCA model, parameters and transition rules chosen are very simple, and they can be obtained with a minimum of field sampling because most of information needed can be searched from previous studies. In spite of its simplicity, the model allowed us to draw some novel theoretical and applied hints on the invasion processes. Results of the IMCA application will help to design the optimal management for the conservation of native species populations while preventing and controlling invasions. Main applications are

related to a better knowledge of traits conferring invasiveness, which will allow to design more effective screening programs for introduction policies, and a better understanding of species and habitat interactions for preventing invasions and controlling already established invaders.

Acknowledgements

The authors wish to thank fruitful discussions with M. Gillman. We wish to thak fruitful suggestions from anonymous reviewers that allowed an improvement of the work. This research was supported by grants from Secyt - Universidad Nacional de Córdoba, Agencia Córdoba Ciencia and CONICET (Argentina).

References

[1] D. E. Elton, The ecology of invasions by animals and plants, Methuen and Company, London (1958) .

[2] W. M. Lonsdale, Global patterns of plant invasions and the concept of invasibility, Ecology 80 (1999) 1522-1536.

[3] Alpert, E. Bone & C. Holzapfel, Invasiveness, invasibility and the role of environmental stress in the spread of non-native plants, Perspectives in Plant Ecology, Evolution and Systematics 3 (2000) 52-66.

[4] A. Okubo, P.K. Maini, M.H. Williamson & J.D. Murray, (1989) On the spatial spread of the grey squirrel in Britain, Proceedings of the Royal Society, London, Series B 238 (1989) 113-125.

[5] L.R. Walker & P.M. Vitousek, An invader alters germination and growth of a native dominant tree in Hawaii, Ecology 72 (1991) 1449-1455.

[6] M. Gilpin, Ecological prediction, Science, 248 (1990) 88-89.

[7] S.I. Higgins & D.M. Richardson, A review of models of alien plant spread, Ecological Modelling 87 (1996) 249-265.

[8] J.G. Skellam, Random dispersal in theoretical populations, Biometrika 38 (1951) 196-218.

[9] A. Okubo, Diffusion and ecological problems: Mathematical models, Springer-Verlag, Berlin (1980).

[10] D.E. Marco & S.A. Páez, Invasion of *Gleditsia triacanthos* in *Lithraea ternifolia* montane forests of central Argentina, Environmental Management 26 (2000) 409-419.

[11] S.I. Higgins, D.M. Richardson & R.M. Cowling, Modelling invasive plant spread: The role of plant-environment interactions and model structure, Ecology 77 (1996) 2043-2054.

[12] S.I. Higgins, D.M. Richardson & R.M. Cowling, Using a dynamic landscape model for planning the management of alien plant invasions, Ecological Applications 10 (2000) 1833-1848.

[13] J. Wallinga, The role of space in plant population dynamics: annual weeds as an example, Oikos 74 (1995) 377-383.

[14] F. Jeltsch, S. J. Milton, W. R. J. Dean & N. van Rooyen, Analysing shrub encroachment in the southern Kalahari: a grid-based modelling approach, Journal of Ecology 34 (1997) 1497-1508.

[15] S.A. Cannas , S.A. Páez & D. E. Marco, Modeling plant spread in forest ecology using cellular automata, Computer Physics Communications 121-122 (1999) 131-135.

[16] J.M. Keegan, Crecimiento individual, estructura y dinámica poblacional de *Fagara coco* (Gill) Engl y *Lithraea ternifolia* (Gill) Barkley, Rom en un área perturbada de las Sierras Chicas de Córdoba. Thesis, Universidad Nacional de Córdoba, Córdoba, Argentina (1984).

[17] J.W. Silvertown & J. Lovett Doust, Introduction to Plant Population Biology, Cambridge, University Press: Blackwell Science (1993).

[18] M.G. Neubert & H. Caswell, Demography and dispersal: calculation sensitivity analysis of invasion speed for structured populations, Ecology 81 (2000) 1613-1628.

[19] D.R. Hart & R.H. Gardner, A spatial model for the spread of invading organisms subject to competition, J. Math. Biol. 35 (1997) 935-948.

[20] L. Lovett Doust, population dynamics and local specialization in a clonal perennial (*Ranunculus repens*). I. The dynamics of ramets in contrasting habitats, Journal of Ecology 69 (1981) 743-755.

[21] B. M. Bolker & S. W. Pacala, Spatial moment equations for plant competition: understanding spatial strategies and advantages of short dispersal, The American Naturalist 153 (1999) 575-602.

[22] D.E. Marco & S.A. Páez, Soil seed bank of Argentine semi-natural mountain grasslands after cessation of grazing, Mountain Research and Development 20 (2000) 254-261.

[23] M. Kot, M.A. Lewis & P. van den Driessche, Dispersal data and the spread of invading organisms, Ecology 77 (1996) 2027-2042.

[24] F. Takasu, N. Yamamoto, K. Kawaski, K. Togashi & N. Shigesada, Modeling the expansion of an introduced tree disease, Biological Invasions 2 (2000) 141-150.

[25] F. van den Bosch, J.A.J. Metz & O. Diekmann, The velocity of spatial population expansion, J. Math. Biol. 28 (1990) 529-562.

[26] S.I. Higgins & D.M. Richardson, Predicting plant migration rates in a changing world: the role of long-distance dispersal, The American Naturalist 153 (1999) 464-475.

[27] M. Rejmánek & D.M. Richardson, What attributes make some plant species more invasive? Ecology 77 (1996) 1655-1661.

[28] J.L. Harper, Population biology of plants, Academic Press, NY (1977).

[29] J.S. Clark, M. Lewis & L. Horvath, Invasion by extreme: population spread with variation in dispersal and reproduction, The American Naturalist 157 (2001) 537-554.

[30] D.M. Richardson, Forestry trees as invasive aliens, Conservation Biology 12 (1998) 18-26.

[31] P.B. McEvoy & E.M. Coombs, Biological control of plant invaders: regional patterns, field experiments, and structured populations, Ecological Applications 9 (1999) 387-401.

Table 1: Values of life history parameters for the species considered in the model. See text for parameter meanings.

parameter	*G. triacanthos*	*L. ternifolia*	*F. coco*
d [lattice units]	3	1	1
t_{max} [y]	75	140	40
q	0.96	0.98	0.93
t_m [y]	7	20	5
n [seeds/plant]	14000	6000	6000
t_s [y]	1	2	1
f_g	0.2	0.01	0.2
P_s	0.4	0.3	0.5
t_J [y]	5	0	0

Captions for figures

Figure 1: Average population density profiles for *G. triacanthos* spread in a rectangular simulation area of width $L_x = 100$ at three different times.

Figure 2: Average population density profiles for *G. triacanthos* spread in a rectangular area of width $L_x = 100$ *vs.* $\xi = y - Vt$ at four different times, where $V = 1.924$ $grid\ units/year$. Curves collapsing indicate the travelling wave structure of the profiles, while the linear dependency in the semi-log plot at large times correspond to an asymptotic exponential tail.

Figure 3: *G. triacanthos* invasion (black cells) into a dense forest of *L. ternifolia* (grey cells), starting from a line of trees ($t = 0$) located at the bottom of a squared simulation area of 160×160 cells, of homogeneously deep soil. White cells correspond to empty cells.

Figure 4: Average population densities for the invasion process of *G. triacanthos* into the *L. ternifolia* forest as a function of time, in a squared simulation area of 80×80 cells of deep soil.

Figure 5: Average invasion front position $\overline{h}$ of *G. triacanthos* in the dense forest of *L. ternifolia* as a function of time, for a rectangular area of width $L_x = 80$. Velocity of the invasion front (V, measured as the asymptotic speed of the averaged front position $\overline{h}$) is shown, for two different soil states, homogeneously deep soil (continuos line), and homogeneously rocky ground (dotted line).

Figure 6: Average population density profiles for *G. triacanthos* invasion into a dense forest of *L. ternifolia*, starting from a line of trees ($t = 0$) located at the bottom of a rectangular

simulation area of width $L_x = 120$, of homogeneously deep soil, at three different times.

Figure 7: *F. coco* spread (black cells) into a dense forest of *L. ternifolia* (grey cells), starting from a line of trees ($t = 0$) located at the bottom of a squared simulation area of 160×160 cells, of homogeneoulsy deep soil. White cells correspond to empty cells. Different snapshots show consecutive stages of the spreading process, from $t = 20$ years to $t = 2000$ years.

Figure 8: Average population densities for the spread of *F. coco* (dashed line) and *L. ternifolia* (continuous line) forest as a function of time, in a squared simulation area of 80×80 cells of deep soil, starting from different random spatial distribution of both species. The lower and upper curves (black line) correspond to an initial forest composition of 90% and 10% of *L. ternifolia* and *F. coco*, respectively, while the middle curves (grey lines), correspond to 40% and 60% respectively. Other initial proportions lead always to the same final stationary state.

Figure 9: Average invasion front position in a rectangular area of width $L_x = 80$, starting from a line of invaders located at the bottom of the simulation area and a dense forest of natives. Open circles correspond to the IMCA simulation of the *G. triacanthos*-*L. ternifolia* system, while filled triangles correspond to the simulation results for the invasion of *G. triacanthos* in a Non Interacting Model for natives with survival probability $q_n = 0.98$ (same value as for *L. ternifolia*).

Figure 10: Invasion velocity (cell length units per year) as a function of the mean dispersal distance d for different values of the age of reproductive maturity t_m in a rectangular area of width $L_x = 100$. All the rest of the parameters were taken from the *G. triacanthos*-*L. ternifolia* system (see Table 1).

Figure 11: Invasion velocity (cell length units per year) as a function of the mean number of seeds n in normal-log plots, for different values of the product $P_s f_g$, calculated in a rectangular area of width $L_x = 100$. All the rest of the parameters were taken from the *G. triacanthos*-*L. ternifolia* system (see Table 1). (a) V vs n. (b) Plot of the same numerical data as V vs $-nLn(1 - P_s f_g)$.

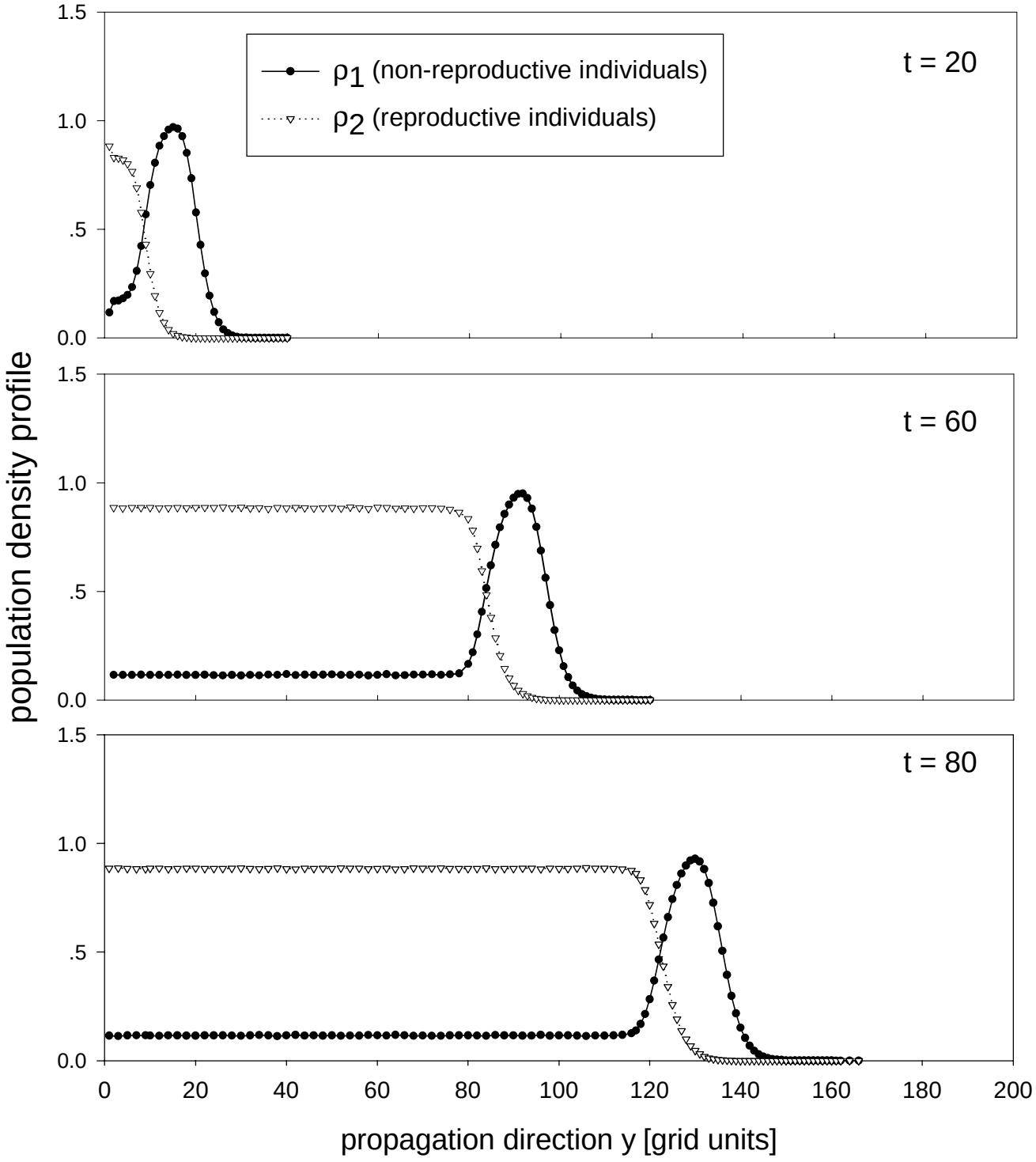

Figure 1- S.A. Cannas et al.

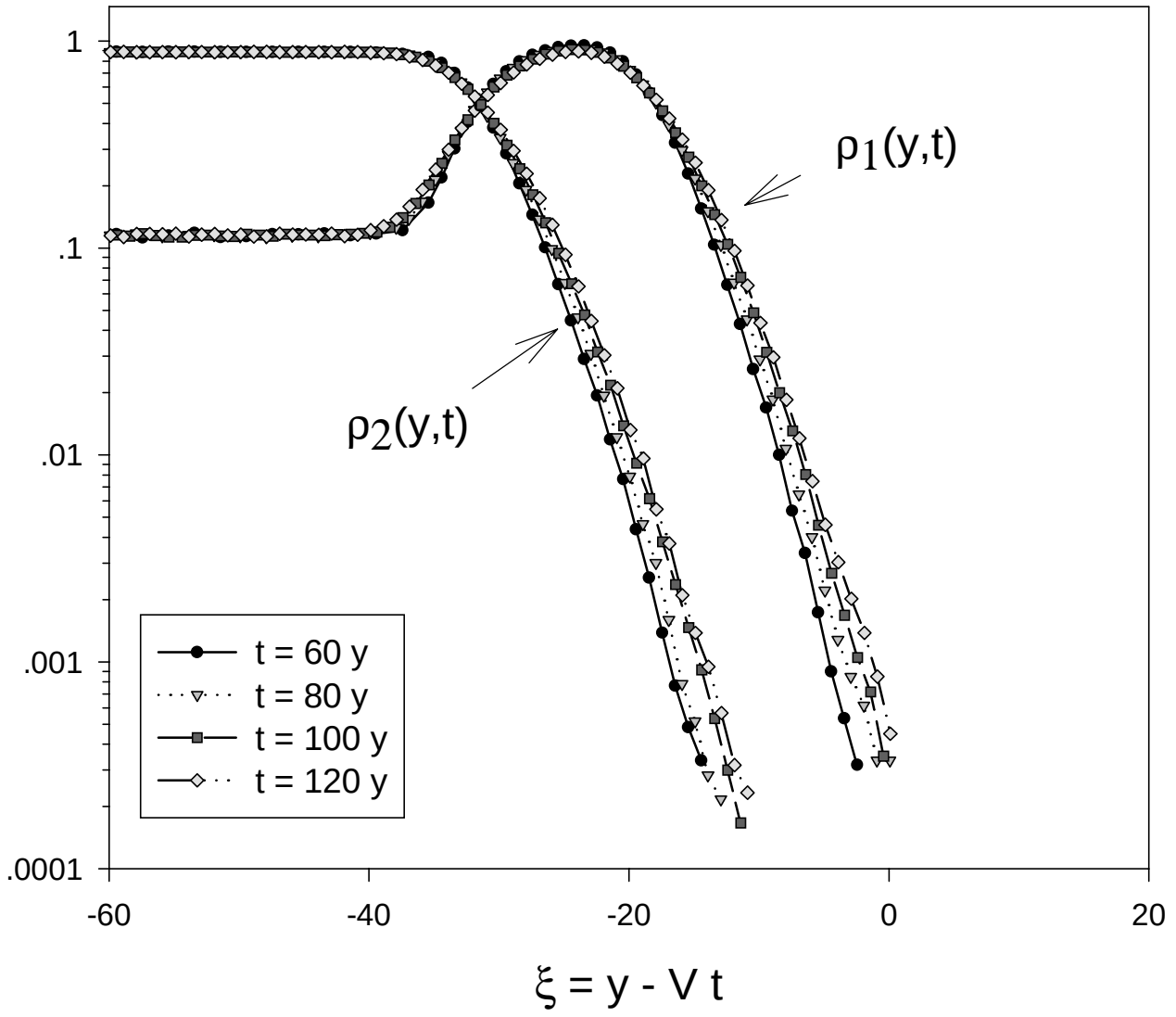

Figure 2 - S.A. Cannas et al.

t=50 y

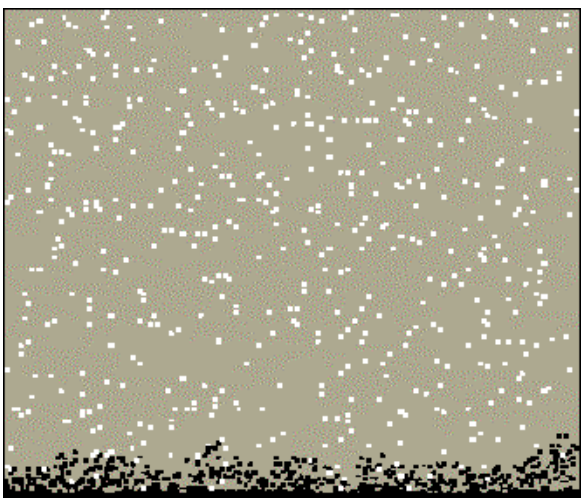

t=200 y

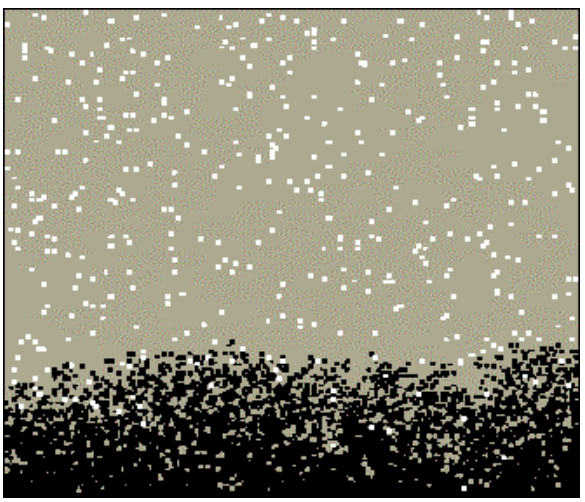

t=100 y

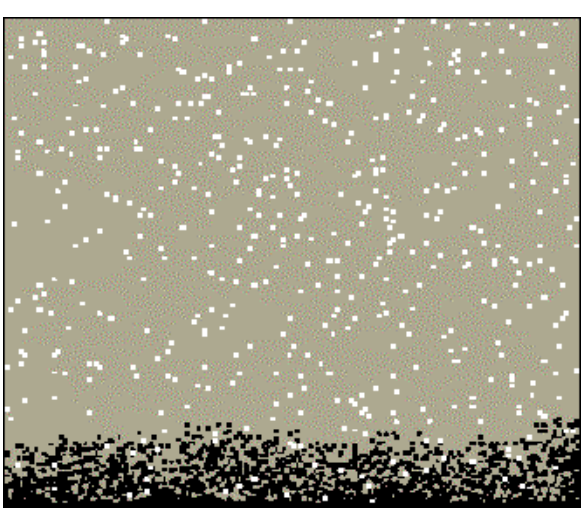

t=350 y

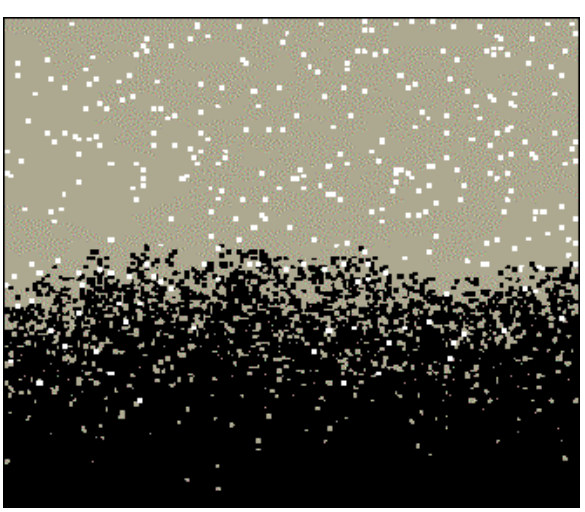

Figure 3 - S.A. Cannas et al.

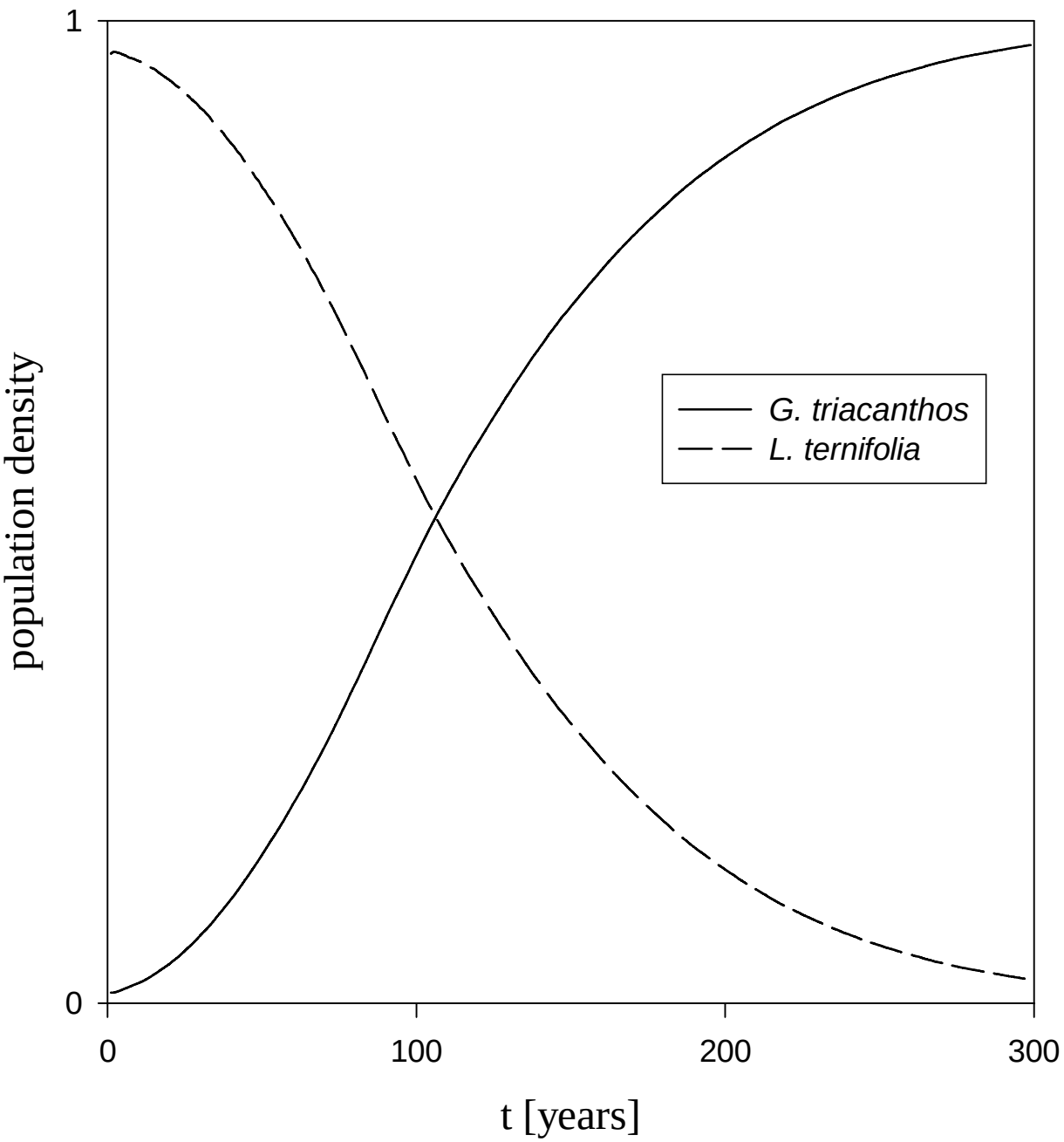

Figure 4 - S.A. Cannas et al.

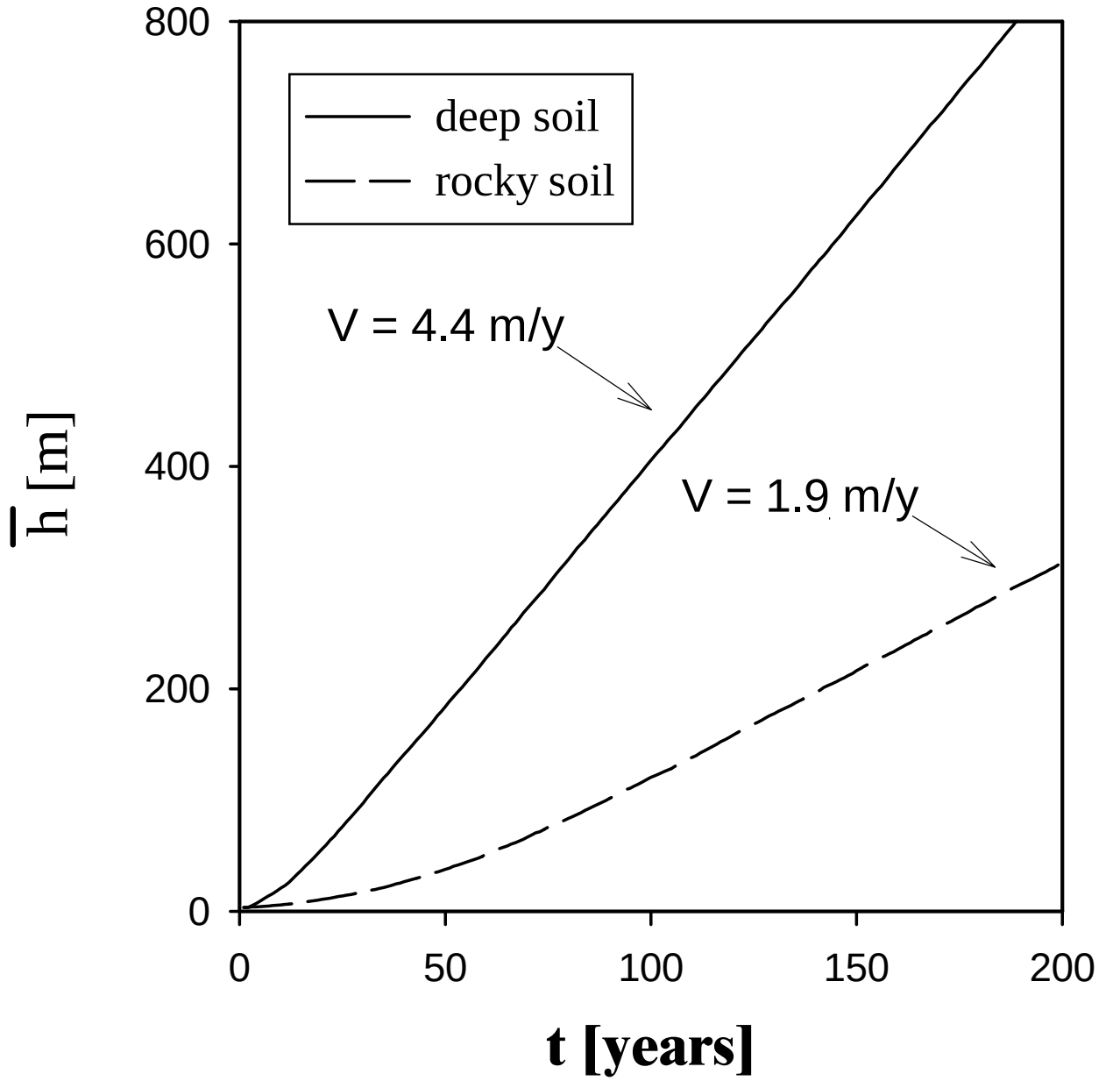

Figure 5 - S.A. Cannas et al.

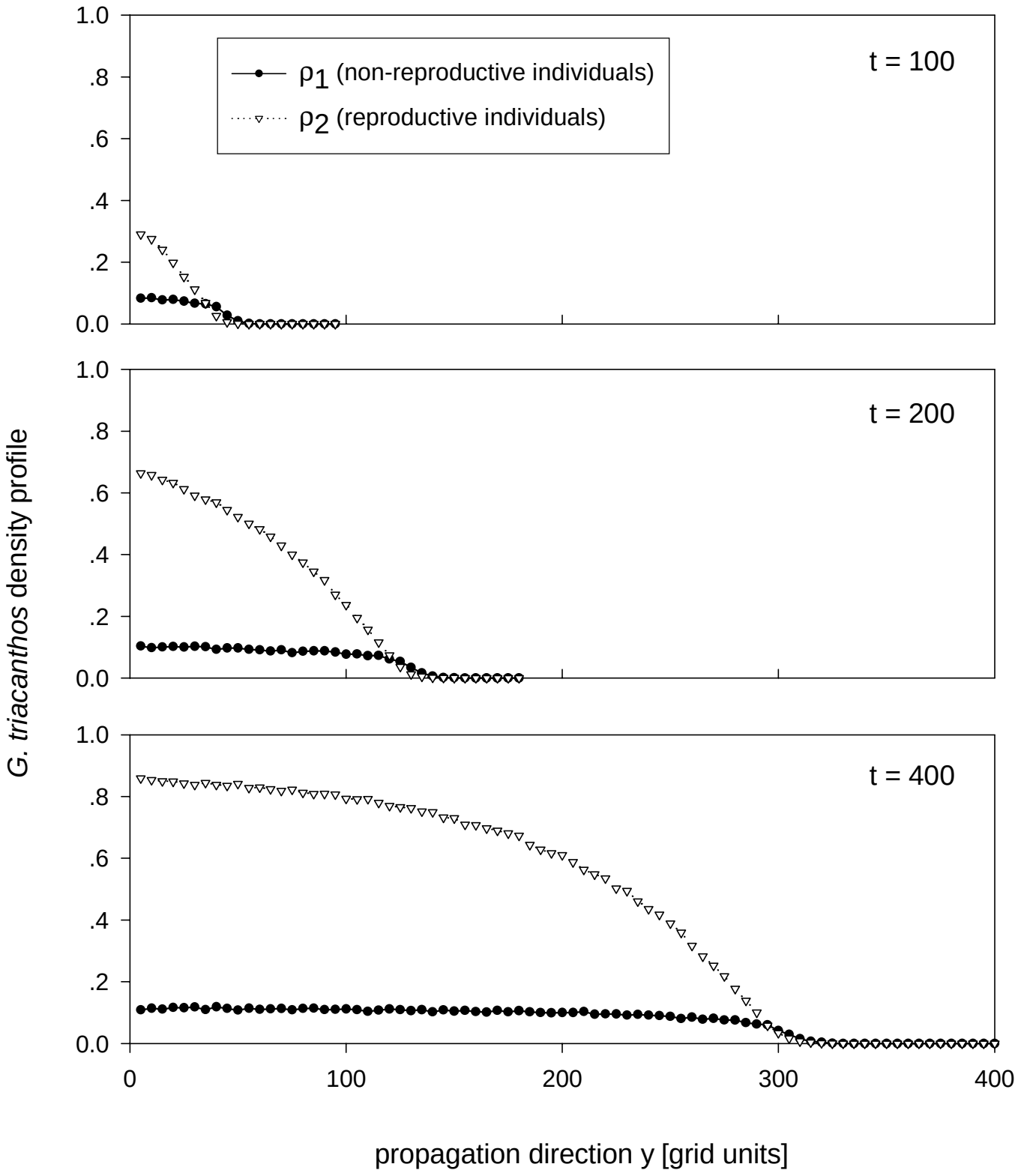

Figure 6 - S.A. Cannas et al.

t=20 y

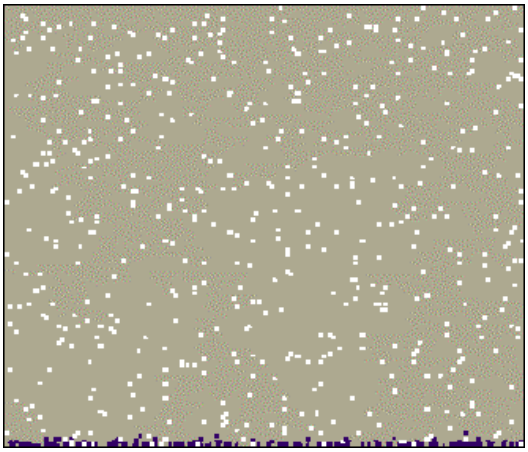

t=500 y

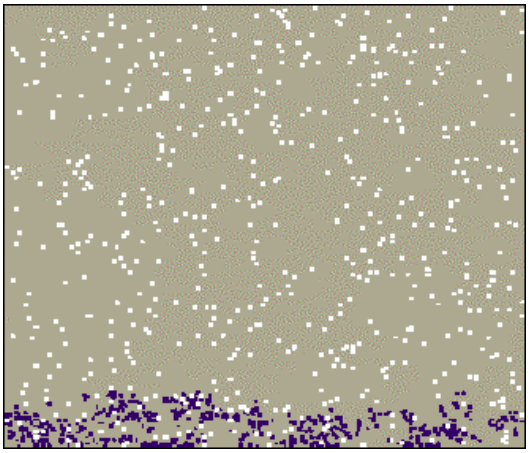

t=100 y

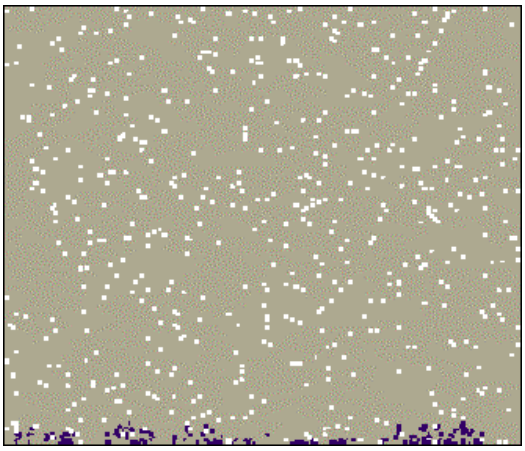

t=1000 y

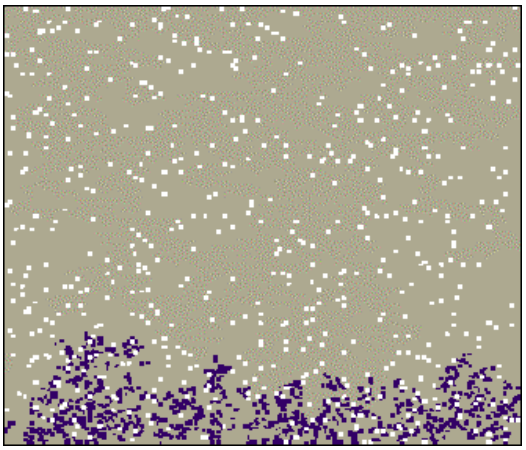

t=200 y

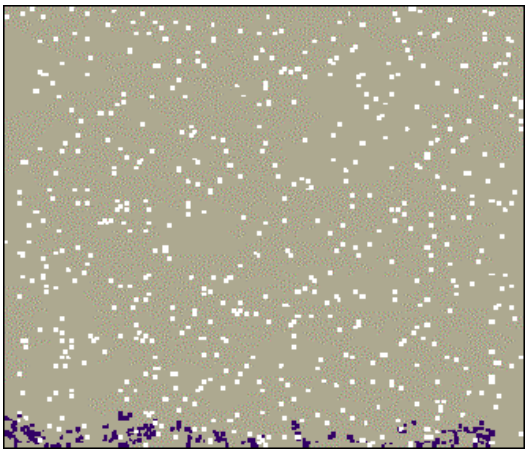

t=2000 y

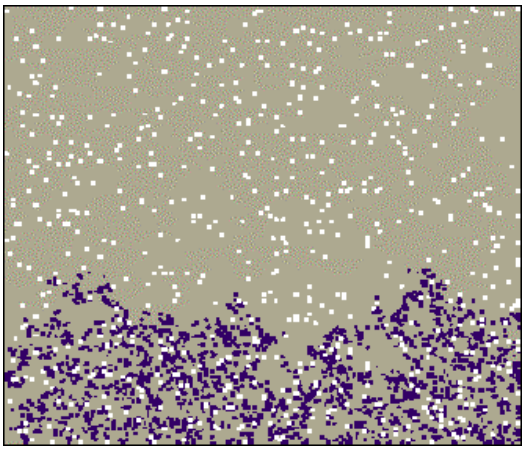

Figure 7 - S.A. Cannas et al.

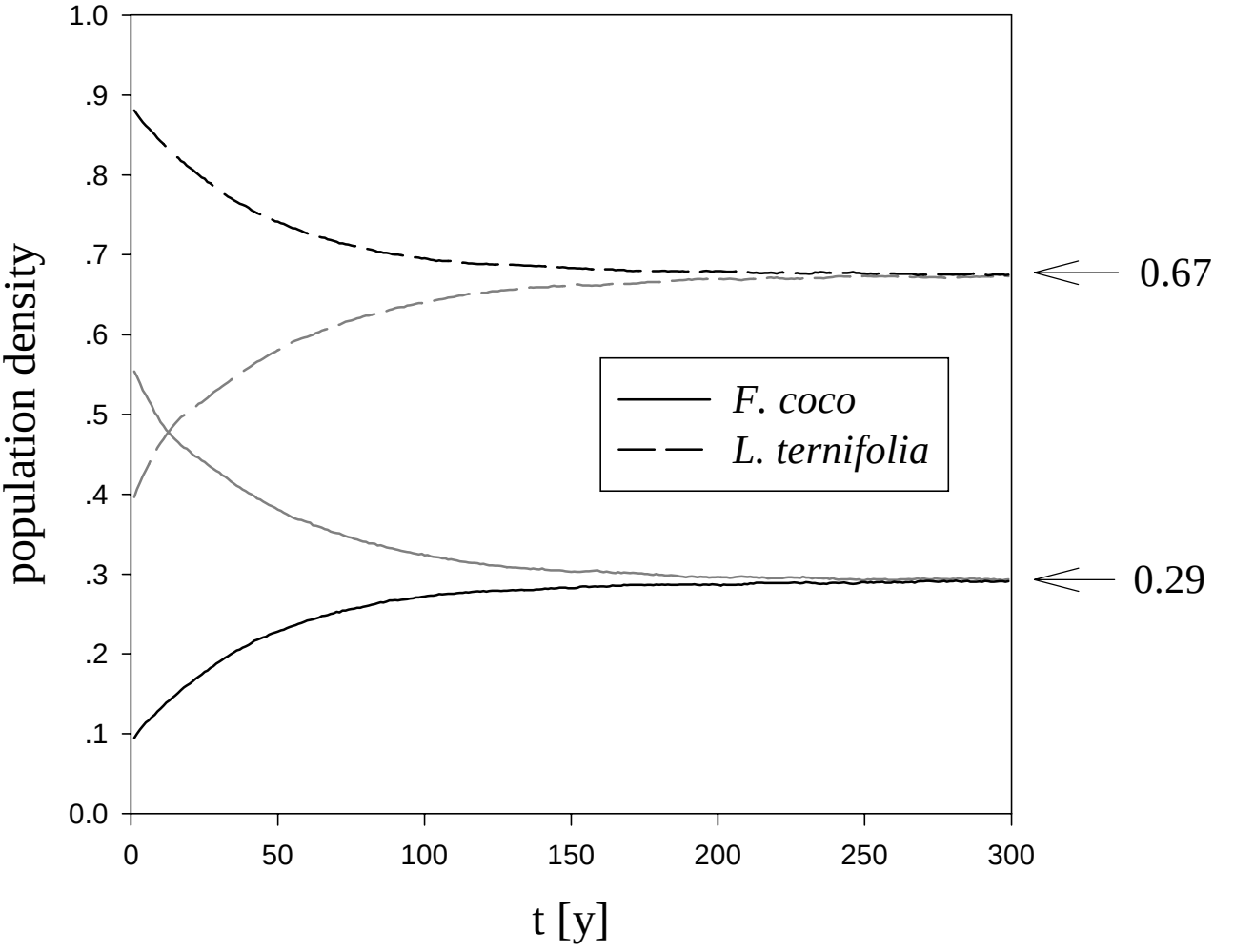

Figure 8 - S.A. Cannas et al.

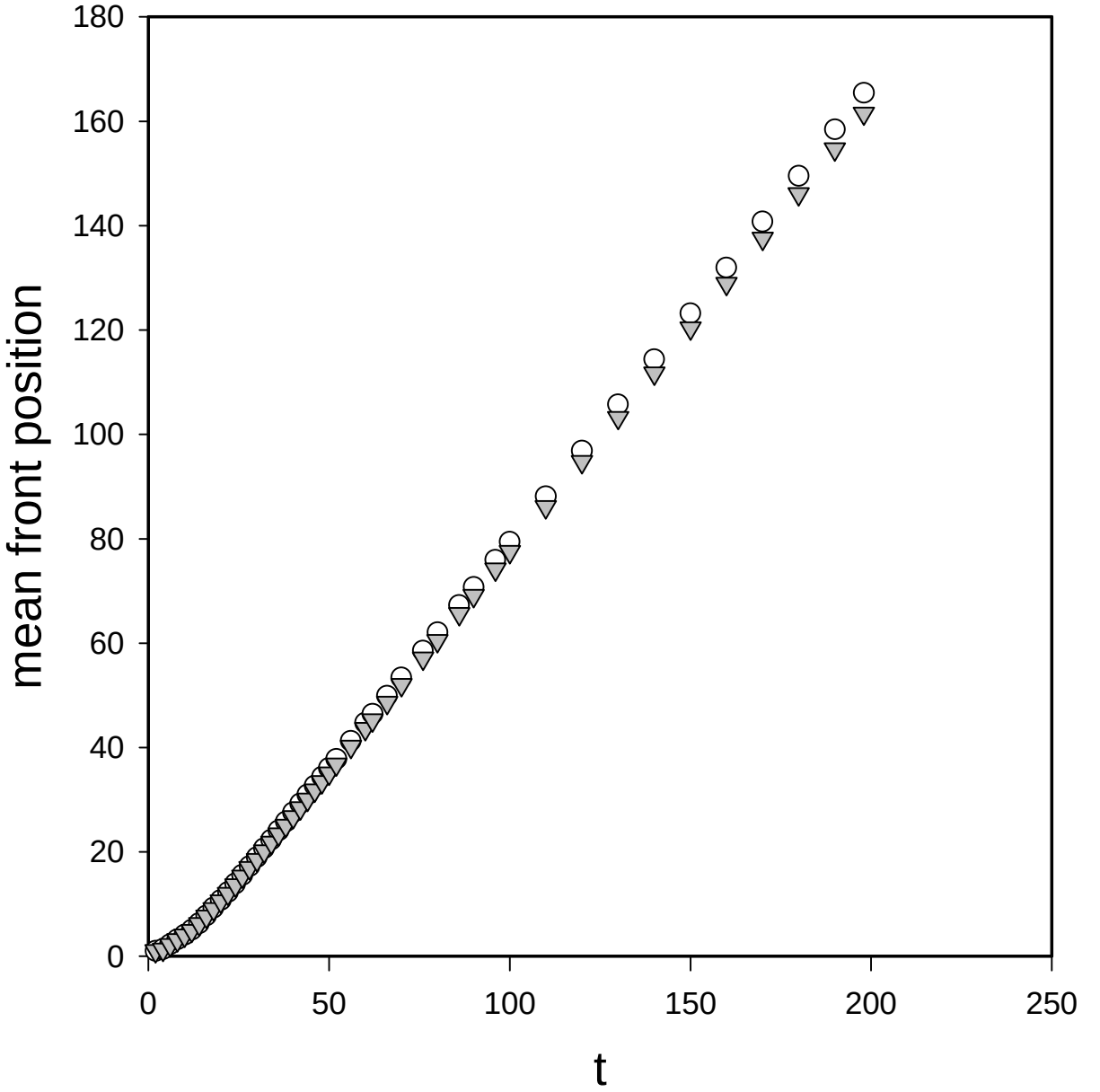

Figure 9 - S.A. Cannas et al.

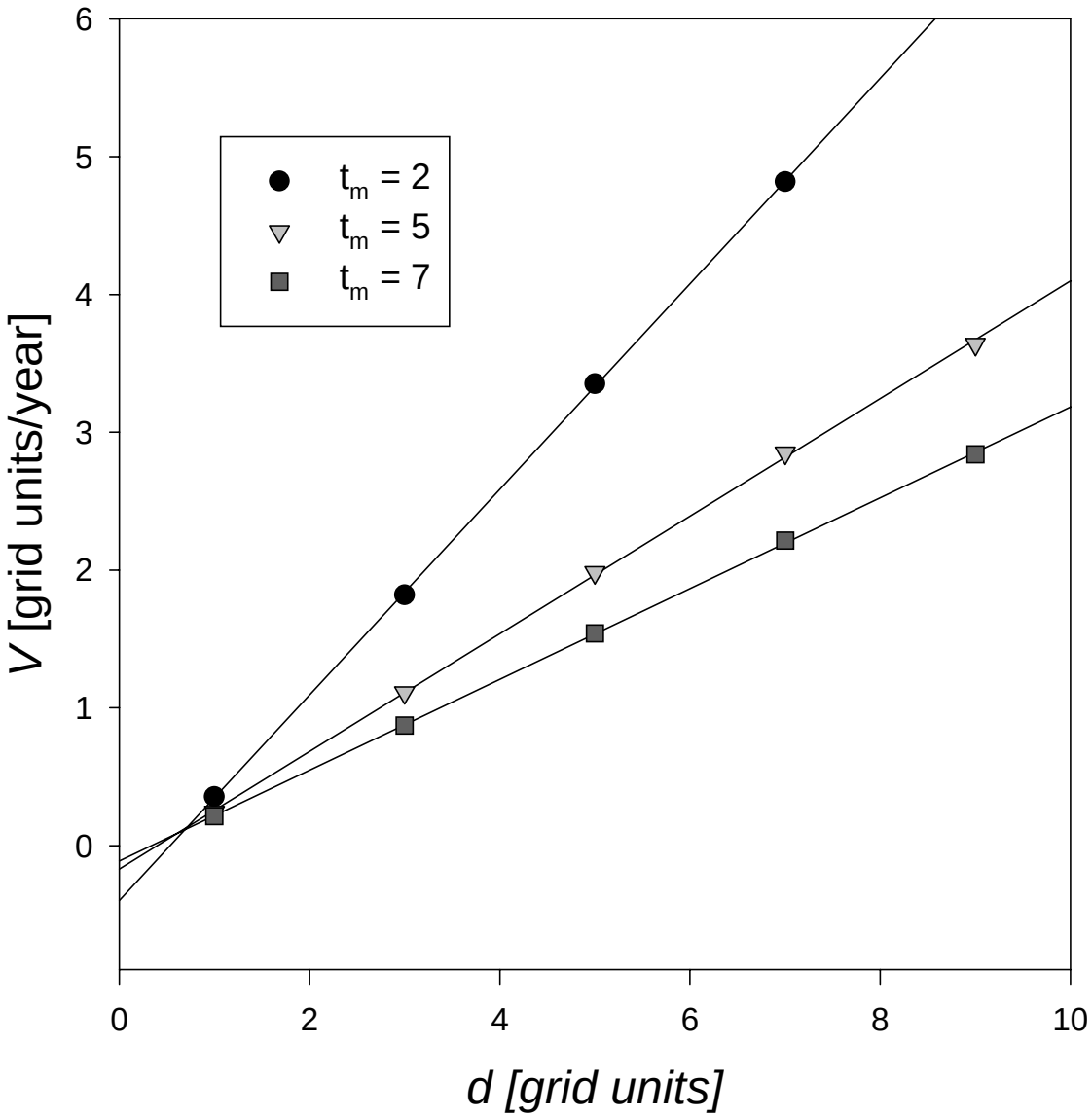

Figure 10 - S.A. Cannas et al.

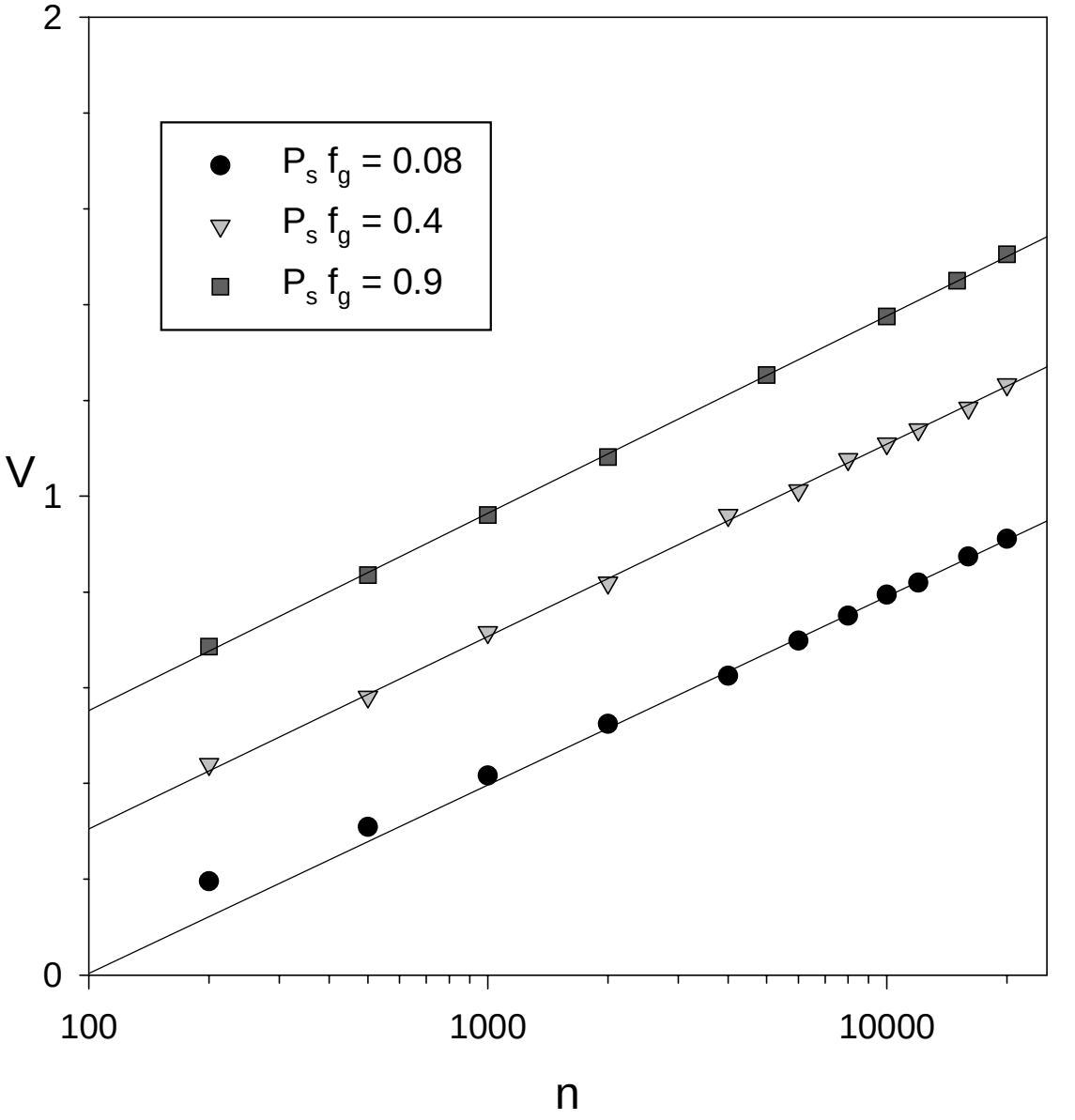

Figure 11a - S.A. Cannas et al.

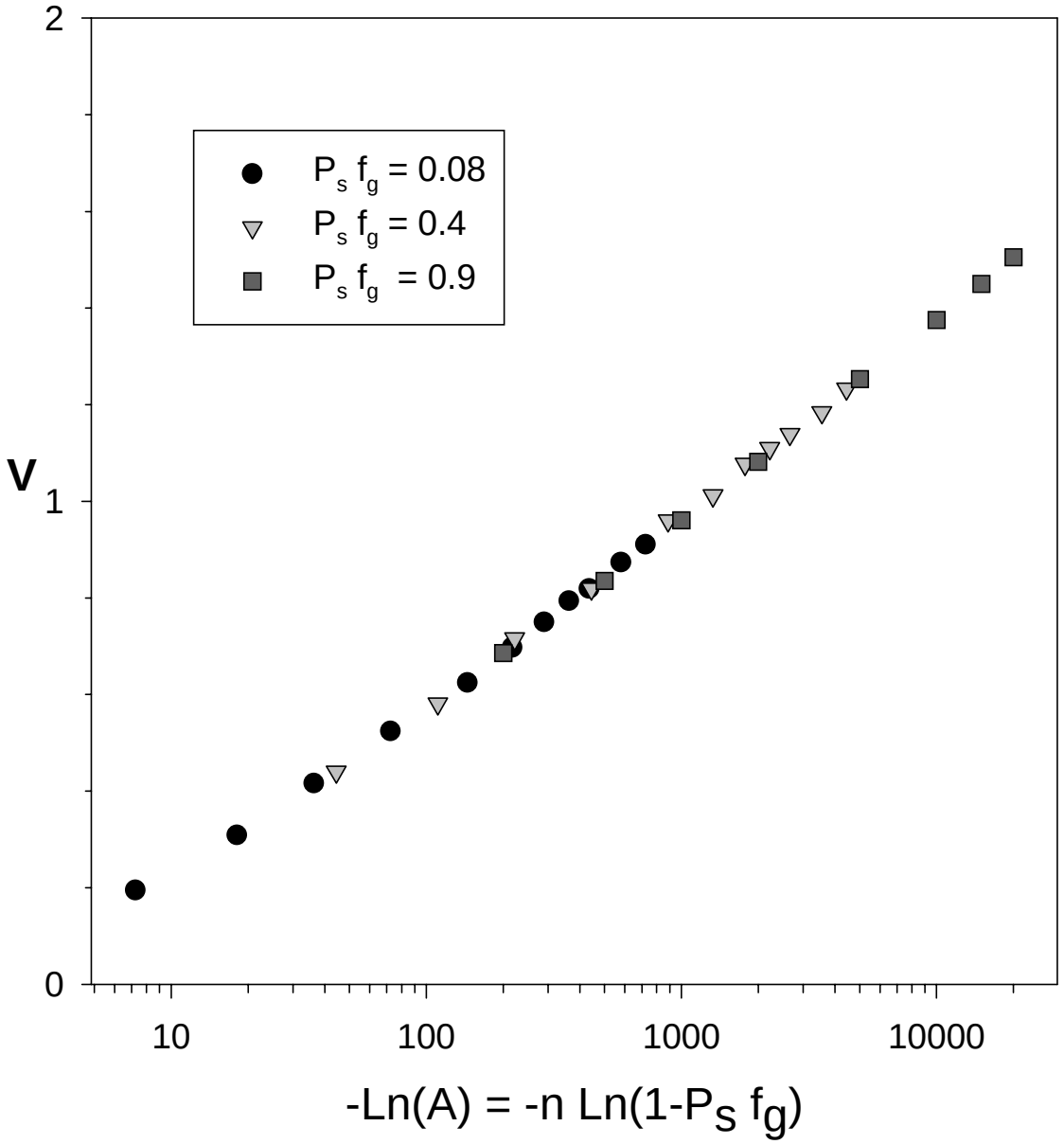

 Figure 11b - S.A. Cannas et al.